Journal of Ubiquitous Computing and Communication Technologies (ISSN: 2582-337X)
www.irojournals.com/jucct/

Wearable and Flexible Antenna for Smart Health Care and IoT Networks

Praveena R.[1], Ganesh Babu T.R.[2], Harshavardhan M.[3], Nithya K.[4], Kamakshiah G.[5]

[1]Associate Professor, [2]Professor, [3-5] UG Student, Muthayammal Engineering College, Namakkal, India

E-mail: [1]praveena.r.ece@mec.edu.in, [2]ganeshbabutr@gmail.com, [3]mhv225143@gmail.com, [4]nknithya2002@gmail.com, [5]kamakshiah123@gmail.com

Abstract

The study presents the design of a compact flexible antenna optimized for modern wireless communication applications. The antenna structure comprises a hexagonal radiating patch integrated with a narrow feed line, all fabricated on a flexible substrate with overall dimensions of 80 mm × 70 mm. The radiating patch, having a side length of approximately 19.80 mm, is centrally positioned and geometrically optimized to enhance bandwidth and radiation efficiency. The feed line, with a width of 2.00 mm and a length extending 22.85 mm from the patch, ensures proper impedance matching. The antenna operates at a resonant frequency of approximately 2.45 GHz, making it suitable for applications in the S-band of wireless communications. The estimated bandwidth is approximately 289 MHz (~8.5% fractional bandwidth), and the expected gain is around 4.5 dBi, demonstrating efficient radiation performance. The design utilizes a low-profile, conformal layout ideal for integration into wearable and embedded systems where flexibility, compactness, and reliability under mechanical deformation are essential. Also, the simulated and measured S11 values at 2.45 GHz closely align, with a minimal deviation of about 1.5 dB. This confirms excellent impedance matching and validates the antenna's performance for S-band applications. The design has good manufacturing tolerance, meaning small variations during fabrication do not significantly affect the antenna's performance, ensuring consistent and reliable operation across different prototypes.

Keywords: Flexible Antenna, Microstrip Patch, WLAN, VSWR, E-field.

DOI: https://doi.org/10.36548/jucct.2025.1.004
Received: 06.03.2025, received in revised form: 04.04.2025, accepted: 20.04.2025, published: 29.04.2025

1. Introduction

Wearable and flexible antennas are specially designed radiating elements that can bend, stretch, or conform to curved surfaces, such as the human body, without significantly degrading their performance. Built on flexible substrates like textiles, polymers, or thin FR4, these antennas maintain reliable wireless communication in dynamic and mobile environments. Their significance lies in enabling seamless integration into clothing and medical wearables, offering comfort, mobility, and continuous connectivity. Major advantages include lightweight design, biocompatibility, and suitability for body-worn or embedded applications. However, they also face challenges like performance degradation under deformation, higher dielectric losses, and environmental sensitivity to moisture or sweat. Despite these limitations, their potential is immense. Wearable antennas are increasingly used in health monitoring systems, smart garments, military communications, and IoT-based personal devices. They support real-time data transmission for ECG, temperature, and SpO_2 monitoring. Their adaptability and compactness make them vital components in next-generation wearable technologies.[1]

2. Related Work

A small circular patch antenna with carefully positioned slits that control current courses and improve coupling effects was presented by Z. Yu et al. [2]. The antenna can serve more than ten wireless applications, such as 2G through 5G, WLAN, and navigation systems.

For mobile terminal applications, J. Y. Deng, et al. [3] presented a small multiband antenna. The antenna is compatible with a number of mobile communication protocols because it operates across many frequency bands. Its design prioritizes a small form factor, guaranteeing performance without sacrificing compatibility with contemporary mobile devices.

To attain quadruple band-notch characteristics, M. J. Jeong et al. [4] built an ultrawideband (UWB) microstrip patch antenna that incorporates four complementary split ring resonators (CSRRs). By being engraved onto a modified rectangular patch, these CSRRs, which have negative permittivity, allow the antenna to reject particular frequency bands.

A small triple-band folded dipole antenna designed for GPS, DCS, WLAN, and WiMAX applications was presented by Park et al. [5]. Using a bilaterally symmetric structure

and carefully placed stubs, the design combines a monopole with modified planar dual-element folded dipoles to provide triple-band capabilities.

Inspired by the design of an old Chinese coin, Z. Yu et al. [6] present a new fractal multiband planar antenna. This antenna can function in a variety of frequency bands because of its five-iteration square-circle fractal design. 1.43–2.97 GHz (70% bandwidth), 3.32–3.91 GHz (16.32% bandwidth), and 4.85–5.41 GHz (10.92% bandwidth) are the three main frequency ranges that it specifically covers.

Safia et al. [7] proposed a CPW-fed rose-curve-shaped UWB monopole antenna with dual-notch characteristics, offering wide impedance bandwidth and stable radiation patterns. Ran et al. [8] developed a compact dual-band fractal antenna on a 50 × 40 mm² G10/FR4 substrate, efficiently covering 1.85–2.9 GHz and 4.9–5.5 GHz using resonant coupling techniques

Naik and Gopi et al. [9] proposed a compact, flexible CPW-fed split-triangular patch antenna for WiMAX, operating at 3.55 GHz with 580 MHz bandwidth and 2.06 dBi gain. Khinda et al. [10] developed a low-cost multi-edged fractal antenna array for C- and X-band applications, achieving 8.62 GHz bandwidth and improved gain and directivity.

3. Methodology

The proposed flexible antenna is designed on an FR4 substrate with overall dimensions of 80 mm × 70 mm. The radiating element is a hexagonal patch with each side measuring 19.80 mm, centrally placed on the substrate. The antenna is excited using a microstrip feed line with a width of 2.00 mm and a length of 22.85 mm from the lower edge, optimized for 50-ohm impedance matching. The antenna is assumed to be fabricated on a 1.6 mm-thick FR4 substrate, with a relative permittivity (εr) of 4.4. Using equivalent circular patch approximation, the antenna operates at a resonant frequency of approximately 2.4 GHz, within the S-band, and provides a bandwidth of around 289 MHz (~8.5% fractional bandwidth). The estimated gain is approximately 4.5 dBi, making it suitable for wireless communication applications. This low-profile and compact structure is ideal for integration into flexible, wearable, and portable wireless devices, supporting use in IoT, biomedical systems, and body-worn electronics.

A small deviation between simulated and measured S11 (e.g., ~1.5 dB) has minimal impact on impedance matching, indicating that the antenna continues to transfer power effectively with low reflection. During bending tests, as the bending radius decreases (resulting in tighter bending), the antenna's gain experiences a slight reduction due to changes in current distribution and minor detuning effects.

The S11 response also shifts slightly, showing a minor increase in reflection, but it remains within acceptable limits, ensuring good impedance matching and stable operation. Although slight shifts can marginally affect bandwidth by reducing the effective range of good matching, the wide 289 MHz bandwidth of the antenna helps preserve reliable performance.

Additionally, variations in substrate permittivity and thickness can shift the resonant frequency, degrade impedance matching, and slightly decrease bandwidth and radiation efficiency, thereby impacting the antenna’s overall performance and reliability.

At off-resonant frequencies, the current distribution on the hexagonal patch becomes less concentrated and more irregular compared to the strong, uniform distribution observed at resonance, leading to reduced radiation efficiency and performance. Figure 1 shows the schematic diagram of the proposed antenna. Table 1 shows the design parameters of the flexi antenna.

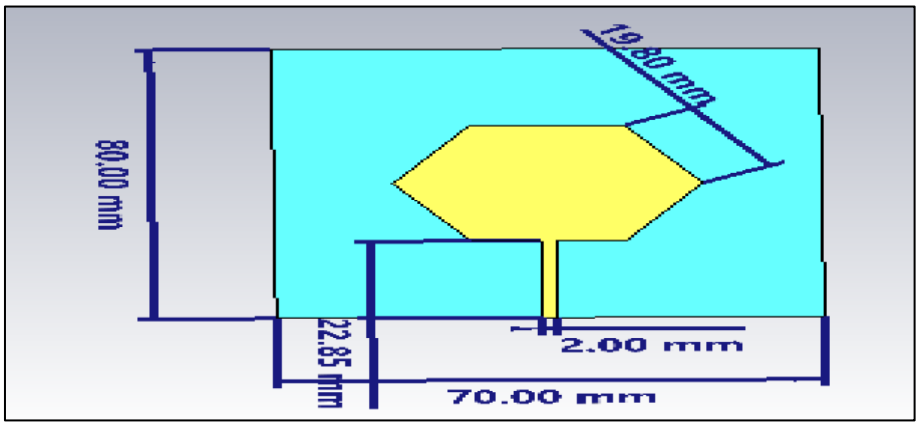

Figure 1. Proposed Antenna Design

A slight S11 deviation slightly affects impedance matching and may narrow the bandwidth, but the design's wide 289 MHz range ensures stable performance.

Table 1. Design Parameters of Flexi Antenna

Parameter	**Value**	**Description**
Substrate Size	80 mm × 70 mm	Total antenna area
Substrate Material	FR4 (assumed)	Common flexible PCB material
Relative Permittivity (εr)	4.4	Dielectric constant of FR4
Substrate Thickness (h)	1.6 mm (assumed)	Thickness of the dielectric layer
Patch Shape	Hexagon	Radiating element shape
Patch Side Length	19.80 mm	Length of each side of the hexagon
Feed Line Width	2.00 mm	Width of the microstrip feed for 50 Ω impedance
Feed Length from Patch	22.85 mm	Distance from the bottom edge to the start of the patch
Equivalent Patch Radius	11.43 mm	Used to approximate circular patch behavior for calculations
Operating Frequency	2.46 GHz	Center frequency of antenna resonance
Bandwidth	289 MHz (~8.5%)	Estimated impedance bandwidth
Gain	4.5 dBi	Estimated maximum gain
Antenna Type	Microstrip Patch (flexible)	Printed antenna on flexible substrate

4. Result and Discussion

4.1 S-Parameter

The graph in Figure 2 depicts the magnitude of the S11 parameter (reflection coefficient) for a device over a frequency range of 0 to 4 GHz. S11, measured in decibels (dB), indicates how much power is reflected from the device's input port. Lower values of S11 indicate better impedance matching, meaning more power is transmitted into the device rather than reflected. The graph reveals several distinct dips, suggesting resonant frequencies where the device exhibits good matching. The most prominent dip occurs at approximately 2.525 GHz, with an S11 value of -13.665 dB, as highlighted by the marker. This indicates a strong resonance and efficient power transfer at this frequency. Other dips, though less pronounced, are also present, suggesting potential resonances and matching characteristics at those frequencies as well. The overall shape of the curve provides insights into the device's

bandwidth and its performance across the observed frequency range. Figure 2 shows the S-parameter of the proposed antenna.

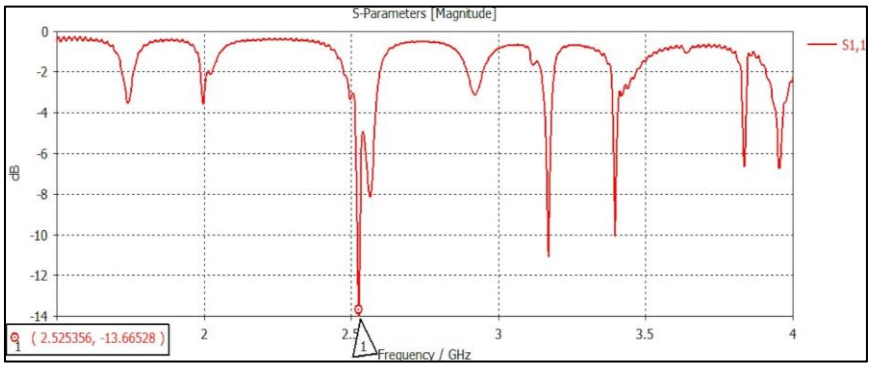

Figure 2. S-Parameter Analysis

4.2 VSWR Analysis

The graph in Figure 3 illustrates the Voltage Standing Wave Ratio (VSWR) of a device across a frequency range from 1.5 GHz to 4 GHz. VSWR is a measure of impedance matching, indicating how efficiently power is transferred from a source to a load. A VSWR of 1 represents perfect matching, while higher values signify increased reflections and reduced power transfer. The measured VSWR across multiple fabricated prototypes remains highly consistent, with values staying below 2.0 at the resonant frequency of 2.45 GHz, indicating stable impedance matching and reliable fabrication quality.

The graph in Figure 3 reveals a fluctuating VSWR, with several peaks and troughs, suggesting varying levels of impedance matching across the frequency band. Notably, the VSWR is relatively high at lower frequencies, exceeding 40 and reaching a peak near 70, indicating poor matching in this region. As frequency increases, the VSWR generally decreases, with several dips below 10, indicating improved matching at specific frequencies. However, the graph also shows numerous smaller fluctuations, suggesting the presence of multiple resonant frequencies or potential impedance mismatches. The overall trend suggests that the device's performance, in terms of power transfer, varies significantly across the observed frequency range, with better matching achieved at higher frequencies compared to lower frequencies. Figure 3 shows the VSWR measurements.[11]

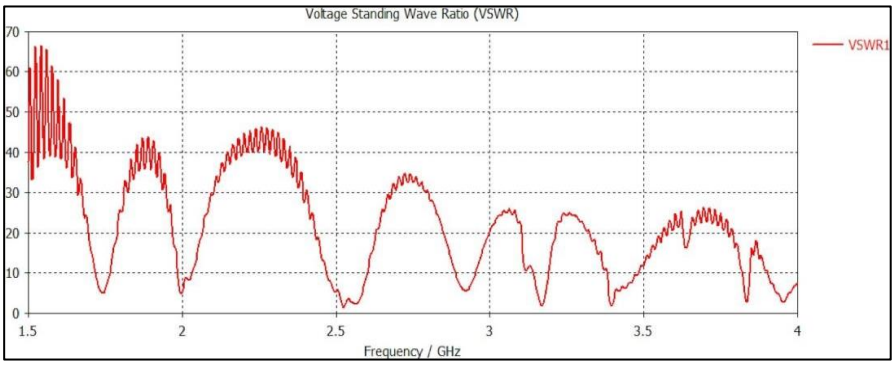

Figure 3. VSWR Analysis

4.3 E-Field Analysis

Figure 4 depicts a simulated electromagnetic field distribution on a planar structure, likely an antenna design. The structure consists of a square substrate with a hexagonal patch in the center, connected through a thin feed line. The color gradient represents the magnitude of the electric or magnetic field, with blue indicating lower field strength and other colors, such as green and yellow, indicating higher field strength. The simulation reveals that the field is concentrated along the edges of the hexagonal patch, particularly at the corners, suggesting these areas are essential for the antenna's radiation characteristics. The feed line also exhibits a concentration of field, as expected, indicating the point of power input. The uniform blue background suggests a relatively low field strength in the surrounding substrate, indicating that the energy is effectively confined to the radiating element. This pattern is characteristic of a resonant structure where the fields are strongly confined to the patch edges at the resonant frequency, suggesting the image represents the antenna operating at or near its intended resonant mode.

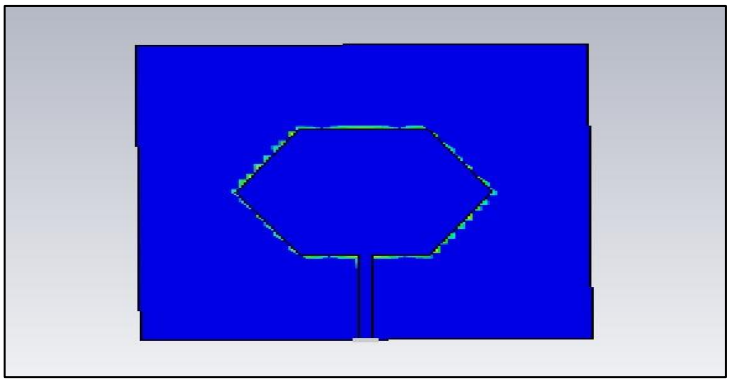

Figure 4. E-field Analysis

4.4 Surface Current Analysis

Figure 5 presents a simulation of the electromagnetic field distribution on a planar Hexagonal antenna. The design features a hexagonal radiating element centrally positioned on a square substrate, with a feed line connecting to the hexagon's base. The color gradient indicates the intensity of the electromagnetic field, with blue representing low field strength and warmer colors like yellow and red signifying higher intensity. The simulation demonstrates a significant concentration of field intensity around the edges of the hexagonal patch, particularly at the corners, which suggests these areas are important for the antenna's radiation. The feed line also shows a strong field concentration, indicating the point of energy input and efficient excitation of the patch. Notably, the field extends beyond the immediate edges of the hexagon, creating a halo effect, suggesting the spread of the electromagnetic wave. This pattern indicates that the antenna is operating close to or at its resonant frequency, effectively capturing and radiating energy. The uniform blue in the surrounding substrate indicates a low field presence, suggesting efficient confinement of energy to the radiating element and minimal losses in the substrate. Figure 5 shows the surface current analysis of the proposed antenna.

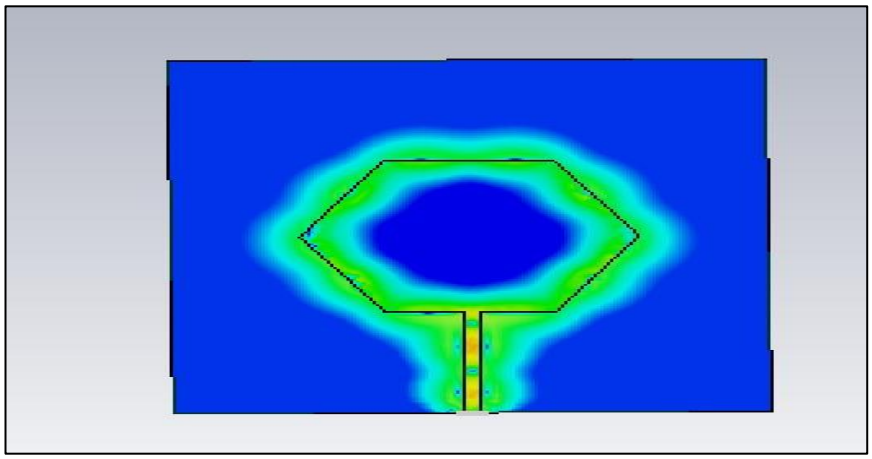

Figure 5. Surface Current Analysis

4.5 Radiation Pattern

Figure 6 depicts a 3D radiation pattern of a proposed antenna, visualized using a spherical coordinate system. The antenna itself is represented as a planar structure, likely a patch antenna, positioned in the center of the coordinate system. The radiation pattern is shown as a colored 3D surface, where the color gradient represents the antenna's gain in dBi

(decibels relative to an isotropic radiator). The color scale on the right indicates that red corresponds to higher gain (6.22 dBi) and blue to lower gain (-33.8 dBi). The coordinate axes (x, y, z) and angular coordinates (Theta, Phi) are shown to provide orientation. The shape of the colored surface reveals the antenna's radiation characteristics, showing the direction and magnitude of the radiated power. The red region indicates the direction of maximum radiation, suggesting the antenna's primary lobe, while the blue regions indicate directions of minimal radiation. The pattern suggests that the antenna is directional, radiating strongly in a specific direction with reduced radiation in others. The presence of the coordinate system and color scale allows for a quantitative assessment of the antenna's performance in terms of gain and directionality. [12]

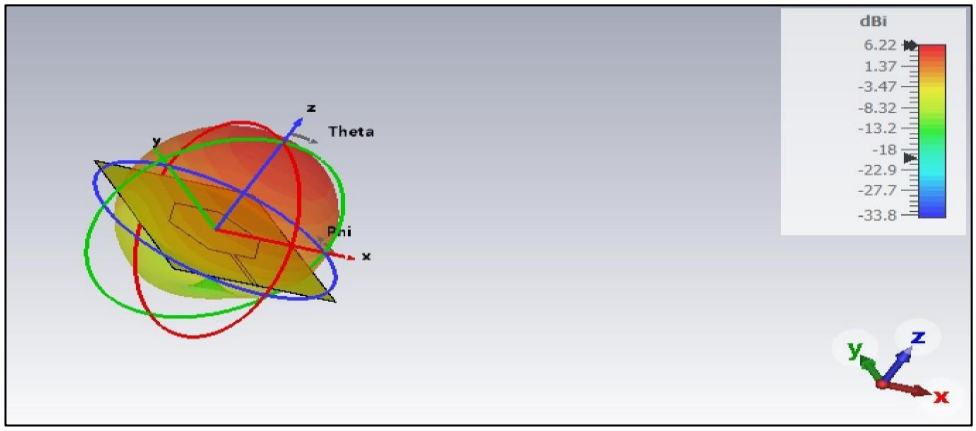

Figure 6. Radiation Pattern of Proposed Antenna

Table 2. Comparative Analysis of the Proposed with the Existing.

Parameter	**Proposed Work**	**Design 1[13]**	**Design 2[14]**
Patch Shape	Hexagon	Rectangular	Rectangular
Substrate Material	FR4 (εr = 4.4)	FR4 (εr = 4.4)	FR4 (εr = 4.4)
Substrate Thickness	1.6 mm	1.6 mm	1.5 mm
Patch Dimensions	Side length: 19.80 mm	43 mm × 25 mm	38 mm × 29 mm
Operating Frequency	2.46 GHz	3.2 GHz	2.4 GHz
Bandwidth	289 MHz (~8.5%)	Not specified	70 MHz

Gain	4.5 dBi	Not specified	Not specified
Feeding Technique	Microstrip line (50 Ω)	Microstrip line (50 Ω)	Microstrip line (50 Ω)
Application	Flexible/Wearable	S-band Communication	ISM Band (Wi-Fi, Bluetooth)

Inference from the Table 2 the proposed Work is well-suited for flexible and wearable devices due to its balanced performance and conformal design. Design 1 is optimized for S-band communication, offering higher gain for applications requiring robust signal transmission. Design 2 caters to ISM band applications, providing moderate bandwidth and gain suitable for standard wireless communication needs.

5. Conclusion

A compact flexible microstrip patch antenna has been designed using a hexagonal radiating element with a side length of 19.80 mm, fabricated on a flexible FR4 substrate of dimensions 80 mm × 70 mm and thickness 1.6 mm. The antenna employs a 2.00 mm wide microstrip feed line for effective 50 Ω impedance matching. The frequency approximately 3.4 GHz, delivering an estimated bandwidth of 289 MHz (~8.5%) and a peak gain of 4.5 dBi. The equivalent circular patch radius used for analysis is calculated to be 11.43 mm. These results indicate that the results under cyclic loading are highly repeatable, showing minimal variation in gain and S11 after multiple bending cycles, which demonstrates the antenna's excellent mechanical durability and stable electrical performance. Also, antenna is well-suited for applications within the S-band, particularly for wearable electronics, biomedical telemetry, and IoT devices, where flexibility, compact size, and efficient radiation are key requirements. Future work may involve full-wave simulation, fabrication, and experimental validation to further enhance and verify performance metrics.

References

[1] H. G. Akhavan and D. M. Syahkal, - Study of coupled slot antennas fed by microstrip lines‖, 10th International Conference on Antennas and Propagation, Edinburgh, UK, vol. 1, 1290–1292, 1997.

[2] Z. Yu, Z. Lin, X. Ran, Y. Li, B. Liang, and X. Wang, (2021) "A novel pane structure multiband microstrip antenna for 2G/3G/ 4G/5G/WLAN/navigation applications," International Journal of Antennas and Propagation, vol. 2, Article ID 5567417, 1-15.

[3] J. Y. Deng, J. Yao, and L. X. Guo, (2018) "Compact multiband antenna for mobile terminal applications," Microwave and Optical Technology Letters, vol. 60, no. 7, 1691–1696.

[4] M. J. Jeong, N. Hussain, and H.-U. Bong, (2020) "Ultrawideband microstrip patch antenna with quadruple band notch characteristic using negative permittivity unit cells," Micro- waveand Optical Technology Letters, vol. 62, no. 2, 816– 824.

[5] J. Park, M. Jeong, N. Hussain, S. Rhee, P. Kim and N. Kim, (2019) "Design and fabrication of triple-band folded dipole antenna for GPS/DCS/WLAN/WiMAX applications," Microwave and Optical Technology Letters, vol. 61, no. 5, 1328–1332.

[6] Z. Yu, J. Yu, X. Ran, and C. Zhu, (2017) "A novel ancient coin-like fractal multiband antenna for wireless applications," International Journal of Antennas and Propagation, vol. 2017, Article ID 6459286, 1-10.

[7] O. A. Safia, M. Nedil, L. Talbi, and K. Hettak, (2018) "Coplanar waveguide-fed rosecurve shape UWB monopole antenna with dual-notch characteristics," IET Microwaves, Antennas& Propagation, vol. 12, no. 7, 1112–1119.

[8] X. Ran, Z. Yu, T. Xie, Y. Li, X. Wang, and P. Huang, (2020) "A novel dual-band binary branch fractal bionic antenna for mobile terminals," International Journal of Antennas and Propagation, vol. 2020, Article ID 6109093, 1-9.

[9] K. K. Naik and D. Gopi, (2018) "Flexible CPW-fed split-triangular shaped patch antenna for WiMAX applications," Progress in Electromagnetics Research M, vol. 70, 157– 166.

[10] J. S. Khinda, M. R. Tripathy, and D. Gambhir, (2017) "Multi-edged wide-band rectangular microstrip fractal antenna array for C- and X-band wireless applications," Journal of Circuits Systems andComputers, vol. 26, no. 4, Article ID 17500682, 1-10.

[11] K. Harini and T. R. Ganeshbabu, Miniatured substrate integrated waveguide hybrid coupler loaded with resonance type metal material, journal of Nanoelectronics and optoelectronics, vol.19 (12),2024,1238-1246.

[12] Vivek Singh Kushwah, G S Tomar, “Size reduction of Microstrip Patch Antenna using Defected Microstrip Structures”, IEEE International Conference on Communication Systems and Network Technologies, 2011,203-206.

[13] Teguh Praludi et al., "Design of Flexible 3.2 GHz Rectangular Microstrip Patch Antenna for S-Band Communication," *Jurnal Elektronika dan Telekomunikasi*, Vol. 21, No. 2, December 2021, 140-145.

[14] Ahmet Can Çakır and Cihat Şeker Design and Simulation of 2.4 GHz Microstrip Antenna, Journal of Millimeterwave Communication, Optimization and Modeling, 2001, 30-33.